Julia sets and chaotic tunneling: I

2009 J. Phys. A: Math. Theor. 42 265101

(http://iopscience.iop.org/1751-8121/42/26/265101)

IOP PUBLISHING JOURNAL OF PHYSICS A: MATHEMATICAL AND THEORETICAL

J. Phys. A: Math. Theor. **42** (2009) 265101 (26pp) doi:10.1088/1751-8113/42/26/265101

Julia sets and chaotic tunneling: I

Akira Shudo[1], **Yutaka Ishii**[2] **and Kensuke S Ikeda**[3]

[1] Department of Physics, Tokyo Metropolitan University, Minami-Osawa, Hachioji, Tokyo 192-0397, Japan
[2] Department of Mathematics, Kyushu University, Ropponmatsu, Fukuoka 810-8560, Japan
[3] Department of Physics, Ritsumeikan University, Noji-higashi 1-1-1, Kusatsu 525-8577, Japan

Received 23 June 2008, in final form 20 January 2009
Published 9 June 2009
Online at stacks.iop.org/JPhysA/42/265101

Abstract

The tunneling phenomenon in non-integrable systems is studied in the framework of complex semiclassical theory. Complex trajectories which dominate tunneling in the presence of chaos (chaotic tunneling) are investigated numerically for several quantum maps. The discovery of a characteristic structure in the initial value representation of tunneling trajectories, named the *Laputa chain*, is reviewed, and it is shown how trajectories starting from Laputa chains make the dominant contribution to the semiclassical calculation of the wavefunction in the chaotic regime. This supports the argument that Laputa chains play an important role in the fully complex-domain semiclassical description of chaotic tunneling. Further, numerical analysis shows that the Laputa chain has distinct asymptotic properties in the long time limit. In particular, it is shown that the imaginary action along the trajectories starting from the Laputa chain, which determines the contribution to the tunneling probability, tends to converge absolutely in the asymptotic limit. On the basis of these features, we propose an empirical definition of the Laputa chain which can provide a basis for further mathematical development. Moreover, a connection is pointed out between the asymptotic structure of Laputa chains and *Julia sets* manifest in asymptotic dynamics of complex maps. Based on these results, we make the conjecture that Julia sets play a fundamental role in the complex semiclassical dynamical theory of tunneling in non-integrable systems.

PACS numbers: 05.45.Mt, 03.65.Sq, 05.45.−a

(Some figures in this article are in colour only in the electronic version)

1. Introduction

A particle in quantum mechanics can penetrate into the region where the transition is strictly forbidden in classical mechanics. Tunneling in quantum mechanics appears as a purely wave

mechanical effect and has no counterpart in classical mechanics. One may thus consider that quantum tunneling is not translatable in terms of the classical mechanics and no connection could be made between purely wave phenomena and particle concepts.

However, if one extends the classical mechanics it is possible to describe even purely quantum phenomena such as tunneling in terms of trajectories. In particular, the extension of classical dynamics to the complex plane is a common and natural way to treat quantum tunneling. A method to construct quantum mechanics exactly in terms of complex trajectories has been proposed by Balian and Bloch [1] and exact quantization using complex periodic orbits has been done by Voros [2]. The instanton method has broadly been applied to evaluate tunneling probabilities [3, 4]. A more sophisticated complex trajectory method was first developed by Miller for the semiclassical description of the multi-dimensional reactive scattering process [5]. However, applications of extended dynamics have been so far restricted to one-dimensional (or effectively one-dimensional) systems whose underlying classical dynamics is simple. The situation is drastically more complicated in systems with more than one dimension in which the motion is not integrable and complicated dynamics due to chaos is generic.

Phase space in non-integrable systems is disjointedly decomposed into infinitely many invariant regions filled with quasiperiodic (rotational) and chaotic orbits. Each invariant set works as a dynamical barrier in classical phase space, while there is nonzero flux in quantum mechanics due to tunneling between them [6]. Recent studies on tunneling in non-integrable systems have revealed that the existence of chaos significantly affects the nature of quantum tunneling. Phenomena observed in purely quantum mechanical calculation of chaotic systems show that tunneling can become *chaotic* [7], or chaos seems to *assist* tunneling [8, 9]. Chaos-assisted tunneling has been observed in cold-atom experiments [10–12] and also in the microwave spectra of superconducting cavities [13]. Furthermore, it has been reported that the emergence of nonlinear resonances, which is a signature of breakdown of integrability, causes enhancement of the tunneling rate [14].

Several efforts have already been made to theoretically describe the rich variety of chaos-assisted tunneling effects. Chaos-assisted tunneling has been explained in terms of a combination of a certain tunneling process through dynamical barriers and the transport process by real chaotic trajectories [15]. It has been shown that sensitive modulation of tunneling splitting under an external perturbation can be well captured by combining an instanton orbit with quantized real space chaos [16].

The combination of instanton theory and quantum perturbation theory also allows the description of novel aspects of tunneling assisted by resonances [14]. These approaches are basically hybrid approaches composed of purely real classical processes (e.g. chaos and/or resonance), and partly complexified classical processes (e.g. instanton) as well as purely quantum processes, in some cases.

In this paper and the following paper ([17], hereafter referred to as part II), we present an approach which allows the description of chaotic tunneling phenomena only in terms of complex classical dynamics. This paper combines and extends the results of a series of earlier papers [18, 19, 21].

In earlier papers [18, 19, 21], we have done extensive semiclassical studies of chaotic maps and found that a particular class of complex paths dominate the tunneling transitions to classically forbidden regions. The dominant paths contributing to the time-domain semiclassical propagator form a set of points having chained structures, named *Laputa chains*, in the plane of initial values. We also showed that the main features of the tunneling wavefunctions in the chaotic systems can be obtained by considering just these chained

structures and gave phenomenological explanations why these structures are significant in chaotic tunneling processes.

This paper aims at giving a clearer specification for the Laputa chain and proposing its definition which fits for further mathematical development. In part II, based on the definition tentatively proposed in this paper, a mathematically more strict definition of the Laputa chain is given and a close connection to the Julia set will be proved.

This paper starts with a description of the method of complexifying semiclassical dynamics which can treat chaotic tunneling in terms of complexified classical paths. Then some examples of Laputa chains, which were found to dominate the chaotic tunneling process [18, 19, 21], are presented together with the reason for them to play special roles in the tunneling process. After reviewing some phenomenological characterization of Laputa chains, we investigate the asymptotic behavior of Laputa chains which exhibit quite remarkable features distinguishing them from other tunneling orbits. These features are used for giving a definition of Laputa chains, and they also lead to an important implication for the close relation between Laputa chains and Julia sets.

Some of the key ideas elaborated in the present and the following paper were presented in our brief preliminary reports [19, 20]. However, due to the limit length of the previous reports, we could not demonstrate the details which are necessary to fully comprehend our observations and arguments. The present paper and the following paper will provide fuller details of our work, in a synergetic approach combining numerical investigations with rigorous mathematical considerations.

In applying the semiclassical method in the complex domain, we inevitably encounter the issue of the Stokes phenomenon in evaluating the quantum propagator semiclassically [22]. The treatment of the Stokes phenomenon requires an additional technicality, which was also developed recently [23].

In this paper we consider the map system. In the flow system, not only the dynamical variables but also time should be complexified, and the latter procedure introduces a specific analytic behavior absent in the map system. Indeed, it was found that the singularity of the trajectories on the complex t-plane plays an important role in the continuous flow problem, which results in the formation of a set similar to the Laputa chain [24].

The organization of this paper is as follows. In section 2, we first introduce the model system used in our analysis. The propagator in the time domain is given both for a fully quantum map and its semiclassical approximation. We introduce a method for representing the complex trajectories in the semiclassical propagator using the initial value representation.

In section 3, we discuss generic features seen in the initial value representation. In particular it is shown that the tunneling trajectories forming the Laputa chain mentioned above dominate the tunneling process. The relation between tunneling components in the wavefunction and the characteristic features of Laputa chains is discussed.

In section 4 we provide numerical evidence that the Laputa chains exhibit a strong tendency of convergence to asymptotic structure in the limit of many iterations. Remarkable features of tunneling trajectories originating in the Laputa chains are also discussed. On the basis of these observed features we give a definition of the Laputa chain. We conjecture that the Laputa chain is strongly connected with the *Julia set*, which is a key notion in the mathematical theory of complex dynamical systems, and present numerical evidence supporting this conjecture.

Part II begins by establishing in section 2 the mathematical relationship between the Laputa chains and the Julia set. The mathematical statements presented there are reexamined by numerical analysis in section 3, and we finally propose a hypothesis which guarantees the existence of tunneling trajectories in non-integrable systems in section 4.

2. Complex semiclassical analysis and tunneling

2.1. The time-domain semiclassical approach

Generic Hamiltonian systems are neither completely integrable nor uniformly hyperbolic. Phase space is filled with quasi-periodic and chaotic regions that are intermingled in a self-similar way. Invariant components are not limited to quasi-periodic and chaotic orbits, but periodic orbits or the orbits on cantori also form invariant sets. Such systems whose phase space is a mixture of infinitely many invariant components are called *mixed systems*. No ergodic component exists such that its support covers the entire phase space and the system is non-hyperbolic in general.

Dynamical tunneling is understood as the transition between different invariant components in classical phase space. For example, congruent tori separated by chaotic regions are connected via tunneling processes. There exist nonzero tunneling couplings between eigenfunctions whose supports are on each torus. This is a typical situation in which dynamical tunneling takes place [6].

In order to relate quantum tunneling with dynamics in classical phase space, it is possible to apply the semiclassical analysis. One may think that the energy-domain argument is most preferred and even canonical as performed in the semiclassical analysis of hyperbolic systems.

We note, however, that this is not always the case in regard to the issue of dynamical tunneling. This is because dynamical tunneling essentially concerns mixed-type systems for which the semiclassical quantization rule in the energy domain has not been established even formally. Rather we should say that the difficulty lies in our ignorance of tunneling processes in mixed phase space. To incorporate the classically forbidden processes, the treatment must include information about invariant sets in the complex phase space. As shown below, it is clear that complex orbits are the most plausible candidates to describe dynamical tunneling, but invariant sets in complex classical phase space are far from well understood. For these reasons, performing the energy-domain semiclassical analysis is not a promising strategy, and hence we here take the time-domain approach.

2.2. Classical maps

The model system we shall study is the so-called kicked rotor model

$$H(q,\, p, t) = H_0(p) + V(q) \sum_n \delta(t - n). \tag{1}$$

Here $H_0(p)$ and $V(q)$ represent the kinetic and potential terms, respectively. The canonical equations of motion induce the two-dimensional area-preserving map from $t = n - 0$ to $t = n + 1 - 0$:

$$g : (p_n, q_n) \longmapsto (H_0'(p_n) - V'(q_n),\ \ q_n + H_0'(p_n - V'(q_n))). \tag{2}$$

Formally we can write the n-step point on the trajectory with the initial condition $(q_0,\, p_0)$ as $(q_n,\, p_n) = g^n(q_0,\, p_0)$.

In the following, we consider three types of maps:

(A) Standard map

$$H_0(p) = \frac{p^2}{2}, \qquad V(q) = K \sin q. \tag{3}$$

Here the parameter K controls the degree of nonlinearity. As far as the real-valued classical dynamics is concerned, it is believed that the standard map captures a generic feature of nearly integrable Hamiltonian systems. In order to see quantum tunneling between the quasiperiodic

and chaotic regions more explicitly, it is more convenient to modify the original standard map into

(B) Modified standard map

$$H_0(p) = \frac{p^2}{2}\frac{(p/p_d)^6}{(p/p_d)^6+1} + \omega p, \qquad V(q) = K\sin q. \tag{4}$$

If $|p| \ll p_d$, we can approximate $H_0(p)$ by ωp, so the corresponding classical map is almost integrable in this domain, whereas for the region $|p| \gg p_d$ the system returns to the standard map. Thus, by taking p_d and K suitably large, we can design the phase space such that an integrable region around the center line $p = 0$ is sandwiched between fully chaotic regions. Then by launching the wavepacket from the initial state

$$\mathcal{A}_\alpha = \{(q, p) : p = 0, 0 \leqslant q \leqslant 2\pi\} \tag{5}$$

we can realize the typical situation of dynamical tunneling in the p-direction from the quasiperiodic region (KAM region) to chaotic seas [18].

The third system that we study most closely here is the system with a cubic polynomial potential.

(C) Hénon map (quadratic map)

$$H_0(p) = \frac{p^2}{2}, \qquad V(q) = aq - \frac{q^3}{3} \tag{6}$$

where a represents a nonlinear parameter. This system can be viewed as a model representing the process of dissociation through a potential barrier, and is suitable for the study of tunneling. An affine change of variables $(q, p) = (y-1, y-x)$ transforms the classical map of the form (2) into a canonical form of the Hénon map

$$f : (x_n, y_n) \longmapsto \left(y_n, y_n^2 + c - x_n\right) \tag{7}$$

where $c = 1 - a$.

The Hénon map is known as the lowest degree polynomial diffeomorphism generating nontrivial dynamics [25, 26]. In particular, the study of its complexified version has made great progress in the last decade [29–32]. Mathematical theory of complex classical dynamics in more than one dimension has been developed only for the Hénon family at present. Our rigorous statements presented in part II will be based on such results, and so are limited only to the Hénon map. However, numerical observations shown below strongly imply that the claims derived in the Hénon map are generalizable to other systems such as the standard map and its modified version as well.

2.3. The quantum propagator in the time domain and its semiclassical approximation

A standard procedure for describing the quantum mechanics of an area-preserving map expresses the time evolution unitary operator in the discretized Feynman path integral form. The one-step unitary operator is given as

$$\hat{U} = \exp\left\{-\frac{\mathrm{i}}{\hbar}H_0(p)\right\}\exp\left\{-\frac{\mathrm{i}}{\hbar}V(q)\right\}. \tag{8}$$

A general formulation of time-domain semiclassics is possible for arbitrary initial states $|\alpha\rangle$ and final states $|\beta\rangle$, but we here choose $|\alpha\rangle$ and $|\beta\rangle$ as the momentum eigenstates because it is most simple and allows intuitive understanding. An alternative choice of $|\alpha\rangle$ and $|\beta\rangle$ will also be made in the case of the Hénon map. The semiclassical formulation for more general choice for $|\alpha\rangle$ and $|\beta\rangle$ will be presented in appendix A.

The n-step quantum propagator for the initial state $p_0 = \alpha$ and final state $p_n = \beta$ is expressed as

$$K_n(\alpha, \beta) = \langle \beta | \hat{U}^n | \alpha \rangle = \int \cdots \int \prod_j \mathrm{d}q_j \prod_j \mathrm{d}p_j \exp\Big[\frac{\mathrm{i}}{\hbar} S(\{q_j\}, \{p_j\})\Big], \quad (9)$$

where $S(\{q_j\}, \{p_j\})$ denotes the action functional along each path

$$S(\{q_j\}, \{p_j\}) = \sum_{j=1}^{n} \big[H_0(p_j) + V(q_{j-1}) + q_{j-1}(p_j - p_{j-1})\big]. \quad (10)$$

The square modulus $|\langle \beta | U^n | \alpha \rangle|^2$ provides the transition probability for transition from an initial state $|\alpha\rangle$ to a final state $|\beta\rangle$.

In the following, we will show how to extend the formulation to include complex trajectories. As is the case of the formulation of full quantum mechanics, the p-representation is used here for the sake of simplicity, but analogous extension to other representations is straightforward (see also appendix A). The semiclassical approximation is to evaluate the multiple integral (9) by the method of stationary phase, the condition of which is given by

$$\frac{\partial S(\{q_j\}, \{p_j\})}{\partial q_j} = 0, \qquad \frac{\partial S(\{q_j\}, \{p_j\})}{\partial p_j} = 0. \quad (11)$$

It is easy to show that the stationary condition is equivalent to the classical mapping rule (2). This is nothing more than the discretized version of the principle of minimum (extremum) action under the constraint that the initial and final momentums are fixed.

The resulting formula which we hereafter call the *semiclassical propagator* is just a discretized version of the Van Vleck–Gutzwiller propagator:

$$K_n^{sc}(\alpha, \beta) = \sum_{\ell} A_n^{(\ell)}(\alpha, \beta) \exp\left\{\frac{\mathrm{i}}{\hbar} S_n^{(\ell)}(\alpha, \beta) + \mathrm{i}\mu^{(\ell)} \frac{\pi}{2}\right\}. \quad (12)$$

The amplitude factor $A_n^{(\ell)}(\alpha, \beta)$ and the classical action $S_n^{(\ell)}(\alpha, \beta)$ are respectively given as

$$A_n^{(\ell)}(\alpha, \beta) = \left[2\pi\hbar \left(\frac{\partial p_n(q_0, p_0)}{\partial q_0}\right)\right]^{-1/2} = \left[2\pi\hbar \left(\frac{\partial^2 S_n^{(\ell)}(\alpha, \beta)}{\partial \alpha \partial \beta}\right)\right]^{-1/2}, \quad (13)$$

$$S_n^{(\ell)}(\alpha, \beta) = S\big(\{p_j^{(\ell)}\}, \{q_j^{(\ell)}\}\big). \quad (14)$$

Note that $\big|A_n^{(\ell)}(\alpha, \beta)\big| \sim \|Dg^n(p, q)\|^{-\frac{1}{2}}$. The suffix ℓ distinguishes different classical orbits each of which satisfies the classical mapping rule (2) with the fixed initial and final boundary conditions $p_0^{(\ell)} = \alpha$ and $p_n^{(\ell)} = \beta$. μ_ℓ denotes the Maslov index and the amplitude factor can also be expressed using the monodoromy matrix for the one-step classical map. Note that $S_n^{(\ell)}(\alpha, \beta)$ is the generating function and should satisfy the relations

$$q_0 = \frac{\partial S_n^{(\ell)}(\alpha, \beta)}{\partial \alpha}, \qquad q_n = -\frac{\partial S_n^{(\ell)}(\alpha, \beta)}{\partial \beta}. \quad (15)$$

If the initial and final states, specified as $p_0 = \alpha$, $p_n = \beta$, are separated by dynamical or energetic barriers, there exist no real classical orbits ℓ starting from the manifold $p_0 = \alpha$ and ending at $p_n = \beta$. The corresponding semiclassical amplitude $K_n^{sc}(\alpha, \beta)$ vanishes and one cannot describe any transition between these two states, although purely quantum wavepackets may penetrate through any barriers.

A standard way to evaluate the tunneling amplitude within the framework of semiclassics is to extend extremum paths to the complex domain. This is achieved by applying the saddle

point method to evaluate the integral (9), instead of the method of the stationary phase. The condition to extract the saddle points is formally the same as (11). Therefore the saddle points thus obtained also satisfy the same classical equations of motion (2) taking into account the boundary conditions $\alpha, \beta \in \mathbb{R}$. These boundary conditions reflect that both p_0 and p_n are observables in the representation under consideration. The semiclassical amplitude also takes formally the same form as (12) but the summation should include not only real classical solutions but also *complex classical trajectories*.

As a particular representation, we focus on the p-representation. In the p-representation, including complex classical trajectories is done by analytically continuing the initial condition of the map (q_0, p_0) to the complex plane. Introducing notations for the initial manifold

$$\mathcal{A}_\alpha = \{(q, p) \in \mathbb{C}^2 : p = \alpha\}, \tag{16}$$

and the final manifold

$$\mathcal{B}_\beta = \{(q, p) \in \mathbb{C}^2 : p = \beta\}, \tag{17}$$

we have a set of the initial points which contribute to the semiclassical propagator (9)

$$\mathcal{M}_n^{\alpha,\beta} \equiv \{(q_0, p_0) \in \mathbb{C}^2 : p_0 = \alpha \text{ and } p_n = \beta\} \tag{18}$$

for given $\alpha, \beta \in \mathbb{R}$, where $(q_n, p_n) = g^n(q_0, p_0)$ according to the definition. Correspondingly, it is convenient to consider the set of end points of the trajectories

$$\mathcal{L}_n^{\alpha,\beta} \equiv \{(q_n, p_n) \in \mathbb{C}^2 : p_0 = \alpha \text{ and } p_n = \beta\}. \tag{19}$$

Note that (q_0, p_0) is uniquely determined for a given (q_n, p_n) since g is invertible. These expressions are available if one replaces the representation of initial and final manifolds by other manifolds. We have only to generalize the initial and final manifolds as

$$\mathcal{A}_\alpha = \{(q, p) \in \mathbb{C}^2 : A(q, p) = \alpha\}, \qquad \mathcal{B}_\beta = \{(q, p) \in \mathbb{C}^2 : B(q, p) = \beta\}, \tag{20}$$

where $A(q, p)$, $B(q, p)$ are classical counterparts of suitable observables, both of which should be given as smooth functions of dynamical variables (q, p). For example, $A(q, p) = a_{pp}p^2/2 + a_{pq}pq + a_{qq}q^2/2$ (action) and $B(q, p) = q$ (position) will be often used in the analysis of the quadratic map. The sets $\mathcal{M}_n^{\alpha,\beta}$ and $\mathcal{L}_n^{\alpha,\beta}$ are then defined by

$$\begin{aligned} \mathcal{M}_n^{\alpha,\beta} &\equiv \{(q_0, p_0) \in \mathbb{C}^2 : A(q_0, p_0) = \alpha \text{ and } B(q_n, p_n) = \beta\}, \\ \mathcal{L}_n^{\alpha,\beta} &\equiv \{(q_n, p_n) \in \mathbb{C}^2 : A(q_0, p_0) = \alpha \text{ and } B(q_n, p_n) = \beta\}. \end{aligned} \tag{21}$$

If α and β are physical quantities to be observed, they should be real-valued.[4]

For the boundary conditions $p_0 = \alpha$ and $p_n = \beta$, the set $\mathcal{M}_n^{\alpha,\beta}$ is expressed using the canonically conjugate initial variable q_0, which in general takes a complex value. Since p_n is a function of q_0 and $p_0 = \alpha$, the set $\mathcal{M}_n^{\alpha,\beta}$ is identified with

$$\{(\xi, \eta) \in \mathbb{R}^2 : p_n(q_0 = \xi + \mathrm{i}\eta, p_0 = \alpha) = \beta\}. \tag{22}$$

For the general boundary condition given by equation (21), $\xi + \mathrm{i}\eta$ should be taken as the variable that canonically conjugate to $A(q, p)$.

To overview all the initial points of the trajectories contributing to the semiclassical summation, it is also useful to scan β from $-\infty$ to ∞. We thus introduce the set of all the initial points landing at the real p_n, which we will denote by $\mathcal{M}_n^\alpha$, and the set of end points of the trajectories leaving $\mathcal{M}_n^\alpha$, which is denoted by $\mathcal{L}_n^\alpha$

$$\mathcal{M}_n^\alpha \equiv \bigcup_{\beta\in\mathbb{R}} \mathcal{M}_n^{\alpha,\beta} = \{(q_0, p_0) \in \mathbb{C}^2 : p_0 = \alpha \text{ and } \mathrm{Im}\, p_n = 0\}, \tag{23}$$

[4] More generally, α and/or β do not necessarily need to be real-valued. For example, if we take the coherent state representation, they become complex.

$$\mathcal{L}_n^{\alpha} \equiv \bigcup_{\beta\in\mathbb{R}} \mathcal{L}_n^{\alpha,\beta} = \{(q_n, p_n) \in \mathbb{C}^2 : p_0 = \alpha \text{ and } \mathrm{Im}\, p_n = 0\}. \tag{24}$$

These are our basic tools for representing the set of initial points and the set of end points which support the time-evolved wavefunctions, respectively.

We make several important remarks concerned with the problem of the Stokes phenomenon in the use of complex semiclassics. In contrast to semiclassics on the real domain, complex trajectories which satisfy the above boundary conditions, *do not necessarily all contribute* to the semiclassical sum. The disappearance of saddle point solutions occurs as a result of the Stokes phenomenon. The Stokes phenomenon is a discontinuous switching of asymptotic solutions of differential equations or saddle point contributions of given integrals. Coping with the Stokes phenomenon is unavoidable when one performs the complex WKB analysis. There may be some optimism that one can deal with this problem in an intuitive manner to remove unphysical divergent parts from the contribution, or that divergent parts can be always identified easily and cut by hand. However, as found in [21], it happens that solutions with weights which are comparable to weights of truly contributing solutions should be removed as a consequence of Stokes phenomenon, which means that without taking into account Stokes phenomenon properly, the semiclassical sum (12) might yield an answer which is not meaningful. The task of extracting a set of correct contributing trajectories out of the candidate trajectories is thus a serious issue. In particular, one cannot in principle avoid this problem in situations where many saddle point solutions inevitably appear. Thanks to the progress of the so-called exact WKB method [2, 33–37] which allows the treatment of asymptotic expansions on the analytical basis via the Borel–Laplace transform, the Stokes phenomenon has become a well-defined concept. On the basis of the exact WKB analysis, especially newly proposed prescriptions for higher order differential equations [38, 39], we are able to handle the Stokes phenomenon at least for the Hénon map with a finite time step [22].

However, this issue is out of the scope of the present paper, and we will not enter into it. Instead, in the following discussion, we apply a phenomenological approach to the Stokes phenomenon, the validity of which has been partly confirmed in [22].

3. Chaotic tunneling and Laputa chains

Our purpose in this section is to show that there exists a specific class of complex orbits which dominate the tunneling process in the presence of chaos. We focus our attention on the case where tunneling proceeds from torus to the chaotic region. This case was reported in detail in our previous papers [18, 22, 21]. In particular, we review the important results discovered using our initial value representation.

3.1. Laputa branches

To begin with, we enumerate *all* the candidate complex orbits. This step looks tedious, but it is inevitable since one does not have any prior knowledge about which complex paths make a large contribution to the semiclassical propagator. The path search is performed by solving a shooting problem: we search for the complex roots $q_0 = \xi + \mathrm{i}\eta$ for a given $p_n = \beta$, and repeat the same procedure by changing β continuously from $-\infty$ to $+\infty$. Then the roots $q_0 = \xi + \mathrm{i}\eta$ move along one-dimensional curves which form the set $\mathcal{M}_n^{\alpha}$.

A difficulty we immediately encounter is that, unlike the path search in the real phase space, the number of complex paths can become infinite even when the time step is finite.

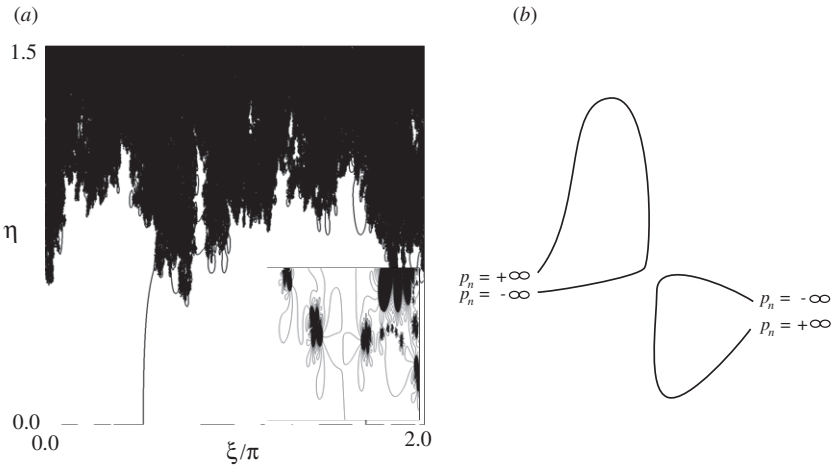

Figure 1. (*a*) A typical example of the set $\mathcal{M}_n^\alpha$ for the modified standard map with $K = 1.2$, $p_d = 5.0$, $\omega = 3.0$ and $n = 14$. The initial wavepacket is placed at $p_0 = 0$. The inset is its magnification. (*b*) Magnification of branches, each of which is a curved open 'string' with two end points.

Indeed, in the case of the standard map, the condition $p_n(q_0, \alpha) = \beta$ at $n = 2$ is explicitly written as

$$\beta = \alpha - V'(\xi + \mathrm{i}\eta) - V'(\xi + \mathrm{i}\eta + \alpha - V'(\xi + \mathrm{i}\eta)). \tag{25}$$

The number of complex solutions for given α and β is infinite due to the transcendental nature of the potential function.

A typical example of the set $\mathcal{M}_n^\alpha$ is shown in figure 1. The set $\mathcal{M}_n^\alpha$ looks as if it were a cloud composed of densely aggregated objects with arbitrarily fine scales. When it is magnified, we recognize the fundamental element of the cloud is a curved open 'string' with two end points (the end points are $\pm\infty$ in some classes of models). We call such a string-like object a *branch*. From the observation of the set $\mathcal{M}_n^\alpha$, we classified the branches into three types.

The first one is just the real axis $\eta = 0$ itself and is called the *real branch*. The orbit launched at the real branch moves only in the real plane, and so the range of $\beta = p_n(q_0, \alpha)$ accessible by such orbits defines the support of the wavefunction reproduced by real semiclassical contributions.

The second and the third types of branch have nonzero imaginary parts and contribute to the tunneling component of the wavefunction. The second type is a branch that intersects vertically with the real branch. The third type is a branch that has no intersections with the real branch. In our previous papers [18, 19, 21], the second type was called the *natural branch*, and the third type was called the *Laputa branch* because it floats in the imaginary domain and reminded us of the Laputa islands in the famous story of *Gullivers' Travels*.

First, we describe two basic features of the Laputa branch based on the results of analytical considerations and extensive numerical observations. The point $q_0^{(c)}$ at which the derivative of the final coordinate vanishes, namely,

$$\left.\frac{\mathrm{d}p_n(q_0, \alpha)}{\mathrm{d}q_0}\right|_{q_0 = q_0^{(c)}} = 0 \tag{26}$$

is called a *caustic*. The two branches should intersect at a caustic because, by the definition, $\mathrm{Im}\, p_n(q_0, \alpha)$ is invariant (recall $\mathrm{Im}\, p_n(q_0, \alpha) = 0$) in the two different directions along the branches at the intersection and equation (26) holds there, but such does not in general occur

in the imaginary domain because the condition $\mathrm{Im}\, p_n(q_0, \alpha) = 0$ is in general incompatible with equation (26). This means that $\mathrm{dRe}\, p_n(q_0, \alpha)/\mathrm{d}q_0$ keeps the same sign along the Laputa branch, and $\beta = \mathrm{Re}\, p_n(q_0, \alpha)$ is a monotonic function of q_0 along it. Extensive numerical observation for various systems reveals the additional feature that $\beta = \mathrm{Re}\, p_n(q_0, \alpha)$ diverges at the two endpoints of the branch. In summary, we claim that

As q_0 moves along a Laputa branch ℓ from one end to the other, $\beta = \mathrm{Re}\, p_n^{\ell}(q_0, \alpha)$ varies monotonically from $-\infty$ to $+\infty$.

Thus each Laputa branch contributes to the wavefunction with the weight

$$\left|\Psi_n^{(\ell)}\right| = \left|A_n^{(\ell)}\right| \exp\left\{-\mathrm{Im}\, S_n^{(\ell)}/\hbar\right\}. \tag{27}$$

It is evident that, in the tunneling problem, the non-vanishing imaginary part of action $S_n^{(\ell)}$ controls the weight in the semiclassical limit $\hbar \to 0$. We remark on a quite general important feature of the imaginary action of the Laputa branch. By the definition, $\mathrm{Im}\, q_n(q_0, \alpha)$ also keeps the same sign along the Laputa branch. (Otherwise, there exists a zero of $\mathrm{Im}\, q_n(q_0, \alpha)$ on the branch, at which (q_n, p_n) as well as $(q_0, p_0) = g^{-n}(q_n, p_n)$ are both real points.) On the other hand, thanks to the generating function property, we have the relation

$$\mathrm{dIm}\, S_n^{(\ell)} \big/ \mathrm{dRe}\, p_n = -\mathrm{Im}\, q_n. \tag{28}$$

Thus $\mathrm{Im}\, S_n^{(\ell)}$ also varies monotonically as q_0 moves along the Laputa branch. Moreover, similarly to $\mathrm{Re}\, p_n$, extensive numerical observations suggest that $\mathrm{Im}\, S_n^{(\ell)}$ also diverges at the two ends of the branch. Taking into account the above relation between q_0 and β, we summarize the behavior of $\mathrm{Im} S_n^{(\ell)}$ along the Laputa branch as

$\mathrm{Im}\, S_n^{(\ell)}$ *varies monotonically from* $\pm\infty$ to $\mp\infty$ *as a function of* $\beta = \mathrm{Re}\, p_n$.

This implies that every branch has a semi-infinite range of β in which $\mathrm{Im}\, S_n^{(\ell)} < 0$. If such a range contributes to the semiclassical propagator, the weight measured by $\mathrm{e}^{-\mathrm{Im} S/\hbar}$ diverges in the semiclassical limit. This is obviously unphysical and there should exist a reason for the removal of such a range. This concerns the Stokes phenomenon and as discussed in [22], we can see that these divergent parts are to be removed. On the other hand, the divergence $\mathrm{Im}\, S_n^{(\ell)} \to +\infty$ is physically reasonable, because the tunneling probability should be null at $|\beta| = \infty$ if n is finite.

The number of potentially contributing orbits is large, but they do not necessarily all contribute with equal weights. If some contributions dominate the others, we need only take into account the dominant contributions and neglect the rest. The next important step is to find a way to identify and select the dominantly contributing complex paths.

3.2. The Laputa chain

In our previous investigations we made an important discovery that there exist characteristic families of trajectories that make dominant contributions in chaotic tunneling. In particular, we analyzed the role of the families of trajectories called *Laputa chains* [18, 19, 21].

A Laputa chain can be identified by its morphological features in the initial value plane. It is a sequence of branches on the set $\mathcal{M}_n^{\alpha}$ with a characteristic appearance, which distinguishes it from other branches. It forms a serial chain-like structure connected via narrow gaps, as shown in figures 2(*a*) and (*b*). Each figure is a magnification of a tiny region in the (ξ, η) plane. One can easily identify a series of branches in a row in the vertical direction, looking like a barbecue skewer. Although it may appear to be a single connected object, the branches are actually separated by narrow gaps. The smallness of the size of the branch forming the chain-like structure is closely related to the exponential sensitivity of trajectories leaving from the branch. At the center of every narrow gap connecting the two adjacent branches a caustic defined by equation (26) always exists. The narrowness of the gap reflects that the caustic is

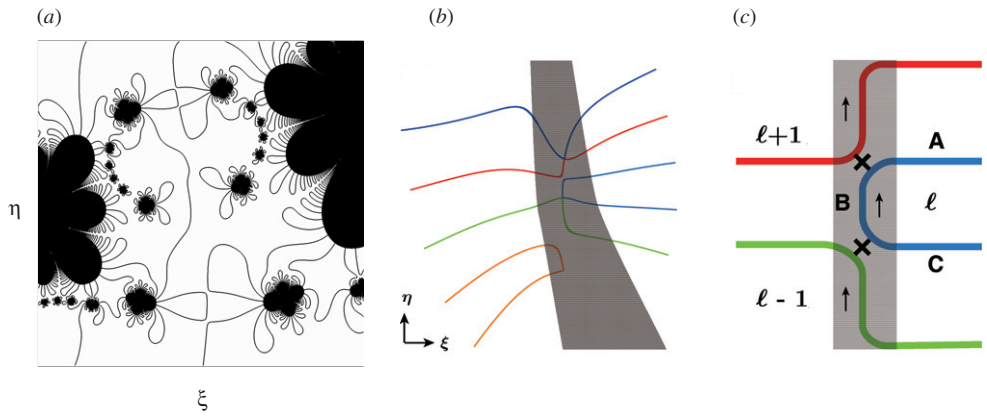

Figure 2. (*a*) An example of the Laputa chain for the modified standard map. The parameters and the initial condition are the same as in figure 1 for $n = 8$. (*b*) An ideal example of the Laputa chain for the quadratic map ($a = 7$). (*c*) A schematic model of the Laputa chain, where only three adjacent branches are shown. The branches are connected by caustics indicated by **X**, and every branch is composed of three parts **A**, **B** and **C**. The series of the part **B** of every branch in the shaded region is regarded as a linked object and is called the 'trunk chain' (see the text).

quasi-real, that is, the trajectory leaving from it lands very close to the real phase plane. The above basic features are described in appendix B in some detail.

The significant role of the Laputa chain becomes apparent when we observe the semiclassical wavefunction obtained by including only branches constituting the Laputa chain. As shown in figure 3, the contributions from the branches forming the Laputa chain have the most dominant weight in the chaotic regime. Close to the classically accessible range of $\beta = \mathrm{Re}\, p_n$ the natural branch dominates the tunneling component, but its contribution drops quickly as β moves away from the classically accessible range, and the most dominant contribution eventually comes from the Laputa chain. Figure 3 shows a typical example exhibiting such a transition process.

Each branch constituting the Laputa chain has a characteristic shape composed of three distinct parts. We denote them as **A**, **B** and **C**, as depicted in figure 2(*b*). The segments **B** are aligned to form a 'necklace' being connected by the caustics. Such a necklace is called the *trunk chain* hereafter because it can be regarded as the main part of the Laputa chain, and a segment **B** is referred to as a *trunk part*, whereas the transversal parts **A** and **C** are each called a *side part*. The segment **B** is characterized as a segment bounded by the quasi-real caustics at both ends. This fact implies that the segment **B** is also quasi-real. Indeed, the trajectory leaving from **B** lands very close to the real plane, namely, $|\mathrm{Im}\, q_n(q_0)| \ll 1$. Quantitative features of the closeness to the real plane will be discussed later in section 3. All the above-mentioned local features are key elements in the phenomenological description of the Laputa chain, as discussed in detail in [18].

We discuss here that Laputa branches are responsible for the formation of a characteristic structure in the tunneling tail of wavefunction. The segment **B** is quasi-real, but, as has been pointed out in section 2.5, $\mathrm{Im}\, q_n$ which keeps the same sign increases rapidly in its magnitude when q_0 comes into **A** or **C** and finally reaches the endpoint. This behavior is schematically shown in figure 4. Recall that $\beta = \mathrm{Re}\, p_n$ varies monotonically as q_0 moves along a branch. Then, the part **B** is mapped to a bounded range of β in which $|\mathrm{Im}\, q_n|$ is very small. Consequently, $\mathrm{Im}\, S_n$ keeps almost the same magnitude from equation (28) in such a range, and thus the semiclassical wavefunction in this range forms a plateau.

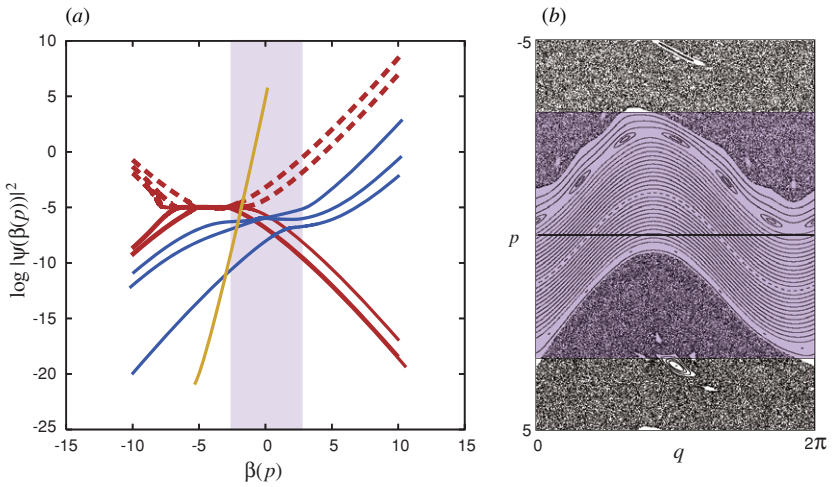

Figure 3. (*a*) Evidence showing that the Laputa chain dominates the rest of the branches. The modified standard map with $K = 1.2$, $p_d = 5.0$, $\omega = 3.0$ is used. The time step is $n = 7$ and the initial wavepacket is placed at $p_0 = 0$. Semiclassical contributions from the Laputa chain (red), a natural branch (yellow) and branches not forming the Laputa branches (blue). Shaded area represents classically regular region $|p| = |\beta| < p_d$ (see equation (4)) in which the initial manifold (16) is taken. The dotted portions of the contributions from the Laputa chain are the parts that should be removed as a result of the Stokes phenomenon. (*b*) The Poincaré map on the real phase space. The shaded region corresponds to the shaded area of (*a*) and the initial manifold $\mathcal{A}_\alpha$ taken in the classically regular region is indicated by the bold line.

We summarize characteristics of the Laputa chain:

Numerical observation (i)

A Laputa chain is a series of Laputa branches connected by quasi-real caustics. 'Quasi-real' means that the trajectory leaving from the concerned point lands very close to the real plane. The dominantly contributing part of the Laputa chain, which is called the turnk chain, is quasi-real and it contributes to the wavefunction with almost the same magnitude, which is observed as the plateau of the tunneling wavefunction characteristic in the chaotic range.

Local analysis around the caustic predicts that a pair of q_0 giving the same $\beta = \mathrm{Re}\, p_n$ face each other across the caustic (see equation (B.3)). Therefore, if one follows a trunk chain from the segment **B** of a branch to that of an adjacent branch jumping over the gap, as is illustrated by the arrows in figure 2(*c*), both $\mathrm{d}\,\mathrm{Re}\, p_n/\mathrm{d}q_0 = \mathrm{d}\beta/\mathrm{d}q_0$ and $\mathrm{Im}\, p_n$ change their signs (this occurs when a caustic is passed; see [18]), the output $\mathrm{Re}\, p_n(q_0) = \beta$ goes back and forth tracing plateaus as indicated in the arrows in figure 4. In other words, for a given β on the plateau, a number of **B** components of the trunk chain contribute to the semiclassical wavefunction. Strictly speaking, $\mathrm{Im}\, S_n^{(\ell)}$ at neighboring **B** s do not take the same values, differing slightly. However, due to the narrowness of the gap (see figure 4), the discrepancy is very small. As a result, all the constituent **B**s contribute to the wavefunction with almost the same weights, and the summed-up wavefunction shows an interference pattern on the plateau range, which is just a feature of the chaotic tunneling tail (see also [18]).

The discovery of the Laputa chain showed that the chaotic tunneling process cannot be described only by a single trajectory, such as an instanton path with a *minimal imaginary action* and an overwhelming weight, nor can it be described by a small number of dominant

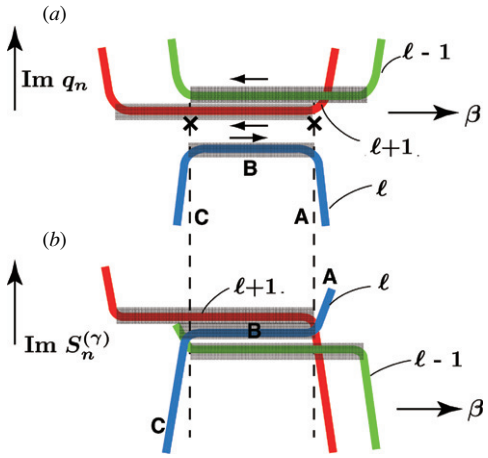

Figure 4. (*a*) Schematic behavior of β versus Imq_n in the three adjacent branches shown in figure 2(*c*). Imq_n takes very small value in the trunk part **B** of each branch. The arrows indicate the directions corresponding to the movement of the input $q_0 = \xi + i\eta$ along the trunk chain in figure 2(*c*). (*b*) The imaginary part of the action Im$S_n^{(\ell)}$ of the three adjacent branches as a function of β. It forms a plateau in the bounded range of β, which corresponds to the quasi-real trunk part **B** of a branch shown in (*a*).

trajectories. Rather, a large number of trajectories are needed to describe chaotic tunneling. It is important to note that the number of the Laputa chains is *not just one*: there are many chains at different spots in the (ξ, η) plane. All the constituent branches in the same chain contribute almost equally to the semiclassical propagator, but contributions from different chains may be different. It is not easy to pick up the most predominant chain at a given $\beta = p_n$ without evaluating their Im $S_n^{(\ell)}$. For example, we do not have any definite criterion to single out the most dominant chain based on features such as location in the (ξ, η) plane or shape.

The number of branches in a Laputa chain increases exponentially with n. In the next section we consider how the contributing branches behave in the asymptotic limit.

4. Asymptotic properties of Laputa chains

As explained in subsection 3.2, a Laputa chain is a family of branches which give dominant contributions necessary for the semiclassical sum to reproduce the quantum wavefunction. In this sense, the Laputa chain is a key object for the chaotic tunneling problem. However, there is no apparent correspondence between the Laputa chain and other known classical dynamical structures. For example, in the energy-domain semiclassical approach, the quantum energy spectra are connected with invariant sets of classical dynamics i.e., the set of the periodic orbits, via trace formula such as the Gutzwiller trace formula [27]. From this point of view, it is important to consider further the correspondence between Laputa chains and generic dynamical concepts. This is our motivation to investigate the asymptotic nature of the Laputa chains in this section.

4.1. Morphological evolution of the Laputa chain

Laputa chains are objects defined at each step n. With increase of n, every branch of the chain splits into finer branches, and the trunk chain shoots out branches of higher generation. After

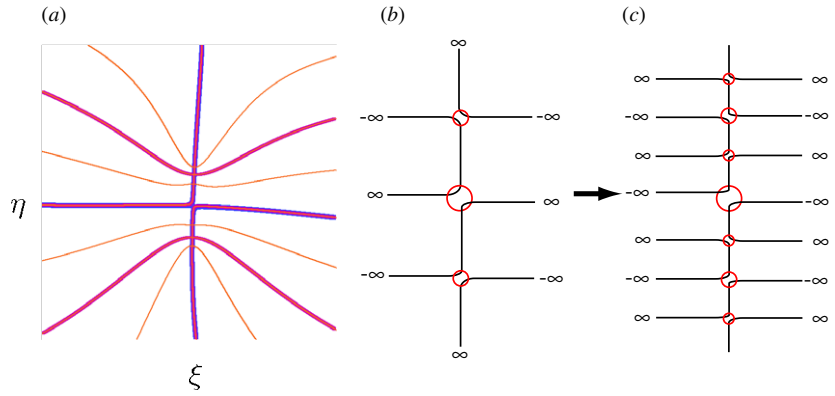

Figure 5. (*a*) Evolution of the Laputa chain when the horseshoe is realized in the real plane ($a = 8.0$) at $n = 4$(blue), $n = 5$(purple) and $n = 6$(red) are superposed. (*b*) Schematic illustration: each branch of the Laputa chain splits into two branches at every step.

sufficiently large n, one can recognize a tendency that the whole chains converge toward a certain asymptotic structure. This suggests that a Laputa chain has an asymptotic limit. Below we present two numerical observations, which characterize the asymptotic nature of Laputa chains.

Numerical observation (ii)

Every branch in the Laputa chain splits in each time step. Such splittings result in the bifurcation of the Laputa chain into a branched structure with higher order chains as the branches. The branches also further bifurcates into higher order branches, and in the limit of $n \to \infty$, the trunk part of the branched Laputa chain, which forms a branched trunk chain, morphologically converges to form a self-similar structure.

The segments **B** are separated by gaps and form the trunk chain. As n increases, the segments **B** further split into finer segments, but they still form a trunk chain. Furthermore the location of the trunk chain becomes fixed as n increases. This fixing of position is a signature of convergence, but especially in the case of non-hyperboic cases, the manner of convergence is neither monotonous nor homogeneous, rather it depends on the position on the trunk chain.

Uniformly hyperbolic cases

In order to show typical features of Laputa chains, we examine the ideal situation realized in the strong nonlinear limit of the Hénon map i.e., $c \ll -1 (a \gg 1)$, in which an ideal horseshoe appears in the real plane and there exists no quasi-periodic region. It is a typical *uniformly hyperbolic situation*, where bounded motions on real phase space occur only on the hyperbolic set.

In figure 5, we show how the Laputa chain evolves with time in the horseshoe case. In every step, each segment **B** splits into two parts and new paired branches appear. As is schematically shown in figure 5(*b*), the number of branches constituting the chain doubles at every step.

Let $\mathcal{T}_n$ be a trunk chain at the nth step. A gap is created when every segment **B** of $\mathcal{T}_n$ splits into two and a new caustic is born there. The location of new **B**s in $\mathcal{T}_{n+1}$ are shifted slightly from that of the old **B**s in the direction transversal to the trunk chain. However, as time

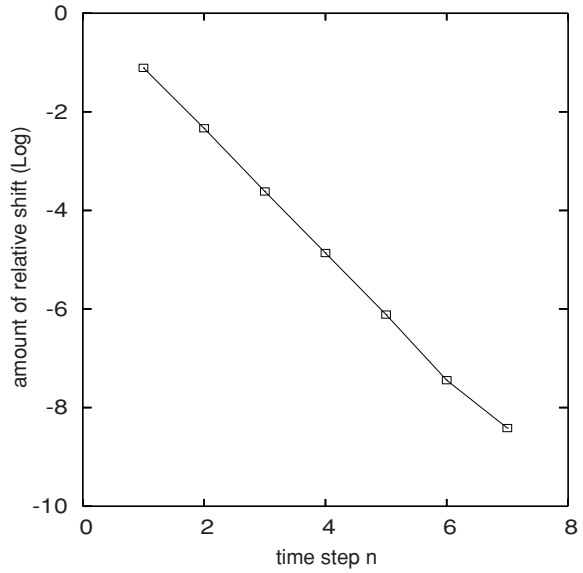

Figure 6. The amount of shift of a trunk part, which is measured by $|q_0^{(n+1)} - q_0^{(n)}|$. The quadratic map with $a = 8.0$ is used.

proceeds, the amount of shift rapidly decreases and the transversal shift of the trunk chain is soon frozen. The freezing process can quantitatively be checked by observing the amount of shift of the trunk part, which is measured by $\left|q_0^{(n+1)} - q_0^{(n)}\right|$ where $q_0^{(n)}$ denotes the intersection of $\mathcal{T}_n$ and some appropriately taken fixed line.

In figure 6, we see nice exponential convergence

$$\lim_{n\to\infty} \left|q_0^{(n+1)} - q_0^{(n)}\right| \sim \mathrm{e}^{-\mathrm{const.}\, n}. \tag{29}$$

Thus there should exist a limit of $q_0^{(n)}$ as $n \to \infty$. The total length of $\mathcal{T}_n$ decreases, but the converged set is by no means empty; it is densely aggregated and forms a Cantor set.

Non-hyperbolic cases

Physically realistic systems are *not* uniformly hyperbolic and the real phase space is a mixture of chaotic and quasi-periodic components. Even in such a case, the splitting of the branches forming the trunk chain occurs, and the location of the split trunk chain also becomes frozen as is observed in the horseshoe case. However, the process is more complicated: the number of splitting is not uniform but changes inhomogeneously depending on both n and the site of the trunk chain. For example, a certain segment **B**, breaks into two for the subsequent five steps, but another **B** splits into three for the subsequent four steps. Nevertheless, it is still common that the split trunk chains tend eventually to an asymptotic structure in the limit of $n \to \infty$.

Furthermore, the splitting into smaller branches occurs on the side part as well as on the trunk part. Once the side part splits, the side part can be regarded as the trunk chain of a new generation. The location of the new trunk chain is frozen in a similar manner to that of the trunk chain. The process repeats successively and trunk chains of new generation are born transversely to the chain of the previous generation, as schematically shown in figure 7(*c*). Thus the limit set is no longer a one-dimensionally arranged sequence, but forms a dendrite

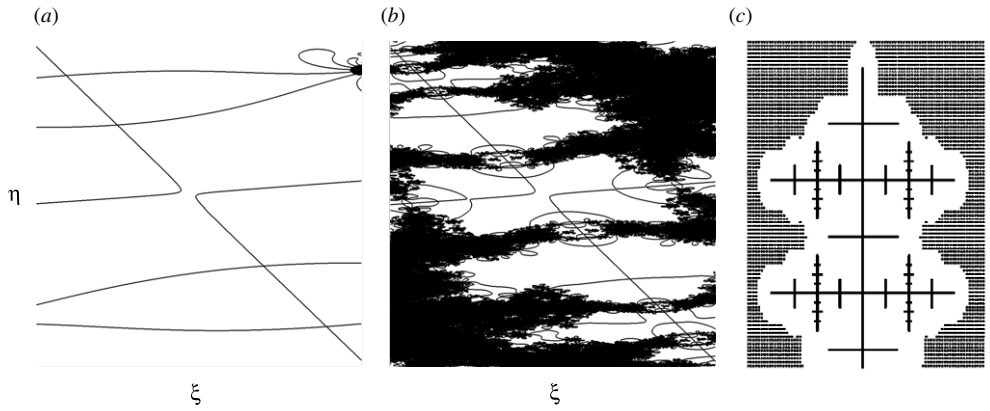

Figure 7. The Laputa chain in the non-hyperbolic case. (*a*) A chain observed at $n = 23$. (*b*) The corresponding chain at $n = 26$. The modified standard map with $p_0 = 0$, $K = 1.2$, $p_d = 5$ and $\omega = 1$ is used. Splitting into finer branches occurs along the side part in the same way as along the trunk part. (*c*) A schematic model for the fully evolved Laputa chain.

pattern with a self-similar structure composed of trunk chains of different generations. Note that the horseshoe limit shown in figure 5 is exceptional in this sense.

4.2. Asymptotic behavior of trajectories starting from Laputa chains

Most branches do not form a Laputa chain, and the end points (q_n, p_n) of the trajectory leaving ordinary branches in general are far away from the real plane, although the boundary condition $\mathrm{Im}\ p_n = 0$ is imposed, which means that $|\mathrm{Im}\, q_n| \gg 1$. In contrast, trajectories launched at the trunk part of Laputa chain end at points very close to the real plane. This is a remarkable feature characterizing the Laputa chain. We here investigate how such a feature is formed with the increase in time steps, paying particular attention to the time evolution of every trajectory. The main result is summarized as below:

Numerical observation (iii)

The itinerary of the trajectories launched from the morphologically converging trunk chain also converges in the limit of $n \to \infty$. *In particular, in the final stage they approach exponentially to the real plane, which means that the imaginary part of action* $\mathrm{Im}\, S_n$ *along the trajectory converges absolutely as* $n \to \infty$.

We are interested not only in the trajectory at a fixed n but also in the asymptotic behavior of the trajectory itself. Figure 8 plots the distance from the real plane as a function of n for the trajectories starting at the points taken on a trunk chain $\mathcal{T}_n$. The horseshoe limit and mixed systems are compared. In either case, we can see that the orbit approaches the real plane *exponentially* in the final stage as is stressed in section 3. With increase of n, the final stage in which the exponential approach is observed is prolonged, and the distance from the real plane at the end point of the trajectory decreases exponetially with n. Moreover, figure 8 implies that there is a strong tendency that the itinerary of every trajectory converges to a certain limit as $n \to \infty$. More precisely, for arbitrary chosen finite step $n_0 (> 1)$, the trajectory (q_j, p_j) from $j = 0$ to $j = n_0$ converges to a limit if $n \to \infty$ is taken.

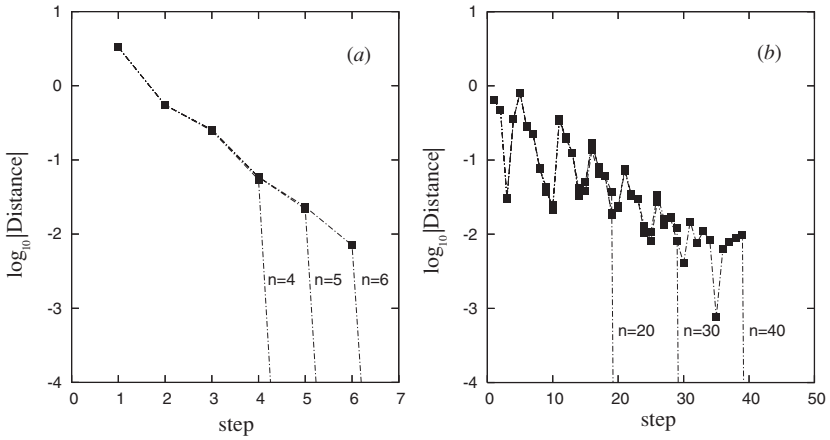

Figure 8. The distance between the real plane and the trajectories launched at the trunks $\mathcal{T}_n$ of increasing n is shown as a function of the step $j(0 \leqslant j \leqslant n)$. (*a*) The horseshoe case, where $n = 4, 5$ and 6 and (*b*) the case of mixed phase space, where $n = 20, 30$ and 40. The quadratic map with $a = 7$ for (*a*) and $a = 0.64$ for (*b*) is used. As n increases, the curves themselves converge so rapidly to an asymptotic limit that they are overlapped and are not distinguishable in this precision. This indicates that the phase space itinerary of the trajectory from $\mathcal{T}_n$ converges very rapidly with n.

This fact strongly suggests that $\mathrm{Im}\, S_n^{(\ell)}$ also converges exponentially to a certain value in the limit $n \to \infty$. To see this more closely, we focus our attention on the element of the action defined by

$$s(q_{k-1}, p_k, p_{k-1}) \equiv H_0(p_k) + V(q_{k-1}) + q_{k-1}(p_k - p_{k-1}). \tag{30}$$

Summation of $s(q_{k-1}, p_k, p_{k-1})$ over k yields the action $S_n^{(\ell)}$. The rapid approach to the real plane implies that the orbit almost obeys the real phase space dynamics in its late stage, and therefore $\mathrm{Im}\, s(q_{k-1}, p_k, p_{k-1})$ also tends quickly to zero. Indeed, we can easily show that, if the dynamics on the real phase space is bounded, there exist certain constants $C_1, C_2, C_3 (> 0)$ such that

$$|\mathrm{Im}\, s(q_{k-1}, p_k, p_{k-1})| < C_1 |\mathrm{Im}\, q_{k-1}| + C_2 |\mathrm{Im}\, p_{k-1}| + C_3 |\mathrm{Im}\, p_k| \tag{31}$$

for sufficiently small $|\mathrm{Im}\, q_{k-1}|$ and $|\mathrm{Im} p_k|$, $|\mathrm{Im}\, p_{k-1}|$. As shown above, the trajectories leaving the series of trunk chains $\mathcal{T}_n (n = 1, 2, \ldots)$ also converge to a fixed trajectory which approaches rapidly to the real plane. Therefore, $\mathrm{Im}\, S_n^{(\ell)}$ along such series of trajectories also converges to a certain definite value in the limit $n \to \infty$. We have to note, on the other hand, that $\mathrm{Re}\, S_n^{(\ell)}$ does not converge because in the late stage the orbit is almost very close to the real phase space. Therefore, $\mathrm{Re}\, S_n^{(\ell)}$ depends sensitively on the final $\beta = p_n$. In this way, $\mathrm{Im}\, S_n^{(\ell)}$ for the trunk chain remains finite even in the limit of $n \to \infty$. Branches other than those contained in Laputa chains exhibit no signature of convergence. $\mathrm{Im}\, S_n^{(\ell)}$s take much larger values than those for the trunk chain, and eventually diverge as $n \to \infty$. There are two possibilities; $\mathrm{Im}\, S_n^{(\ell)} \to +\infty$ and $\mathrm{Im}\, S_n^{(\ell)} \to -\infty$. The contribution of the former case is negligible as compared to that with finite $\mathrm{Im}\, S_n^{(\ell)}$, and the latter trajectories should be removed from the final contribution due to the Stokes phenomenon. This is the main reason why the trunk part of the Laputa chain is the fundamental contributor to the semiclassical propagator.

To summarize this sections and the previous describing asymptotic features of the Laputa chain, we propose here an empirical definition of the Laputa chain on the basis of numerical observations presented so far. Our earlier characterization of the Laputa chain was based only

on morphological features in finite steps [18, 19, 21]. However, there is some ambiguity in its identification, and insufficient for filtering the Laputa chains out of an enormous number of branches forming the set $\mathcal{M}_n^\alpha$. From the numerical observations in previous subsections, we can capture such specific structures especially in terms of their asymptotic nature. Therefore, it is reasonable to define or specify Laputa chains as the subsets of $\mathcal{M}_n^\alpha$ having the following properties.

(1) *They asymptotically converge in shape in the initial value plane.*
(2) *The orbits leaving them approaches the real plane very rapidly.*

We can further replace (2) by the property more crucial to semiclassics as
(2)′ *The imaginary part of action along the trajectories leaving them converge absolutely.*

We propose (1) plus (2) or (1) plus (2') as a more specific and an empirical definition of Laputa chains. We particularly remark that by condition (2) or (2') we filter the trunk part of the chain out of the whole chain, and so we identify the trunk chain with the Laputa chain in the asymptotic limit, which is just mentioned in the numerical observation (iii).

4.3. Extraordinary behavior of trajectories starting from Laputa chains

In this subsection, we present a general feature of dynamics in complex phase space close to the real chaotic region in order to stress that the characteristics of the trajectories launched at the Laputa chains mentioned above are quite unusual. To simplify the situation, we again suppose that the chaotic region is bounded by KAM curves as is the case in the standard or modified standard map.

Let us take an arbitrary initial point P_0 in the complex domain but very close to the real chaotic sea, and also take another point P_0' which is very close to P_0 and located on the real chaotic sea. The distance between the trajectories leaving P_0 and P_0' explodes exponentially with time because of the instability of the chaotic orbits. Since the trajectory from P_0' is confined in real phase space, the instability means that almost all trajectories starting close to the real chaotic seas are repelled from the real plane exponentially.

This argument holds only when the initial point P_0 is sufficiently close to the real plane, and it cannot predict any more about the fate of the repelled trajectories. However, as is shown in figure 9, we can numerically show that almost all the repelled trajectories go further away from the real plane and eventually blow up to infinity. Thus we may say that chaos on the real phase space repels the trajectories in the complex phase space. Such a feature is common in the kicked rotor systems that we have examined. This argument explains why the trajectories launched at 'ordinary' branches end at points far from the real plane although the imposed boundary condition requires $p_n \in \mathbb{R}$. It is then seemingly strange that the trajectories starting at the Laputa trunk are attracted by the real chaotic sea and not repelled from it however large n may be. One hypothesis which can account for this is that the trajectories are on or very close to the complexified stable manifolds of the saddles in the chaotic sea. If this is indeed the case, the complex trajectories starting at the Laputa chain will almost follow the dynamics on the real chaotic region, and never explode to infinity even in the limit of $n \to \infty$ since we here assume the chaotic region is bounded. We therefore reach the following important conjecture: the Laputa trunk chain is a set of initial points whose trajectories are bounded and cannot go to infinity.

4.4. Laputa chains and Julia sets

The *Julia set*, which plays a central role in the theory of complex dynamical systems, is specified as the set that exactly possesses such a property. More precisely, the *forward Julia*

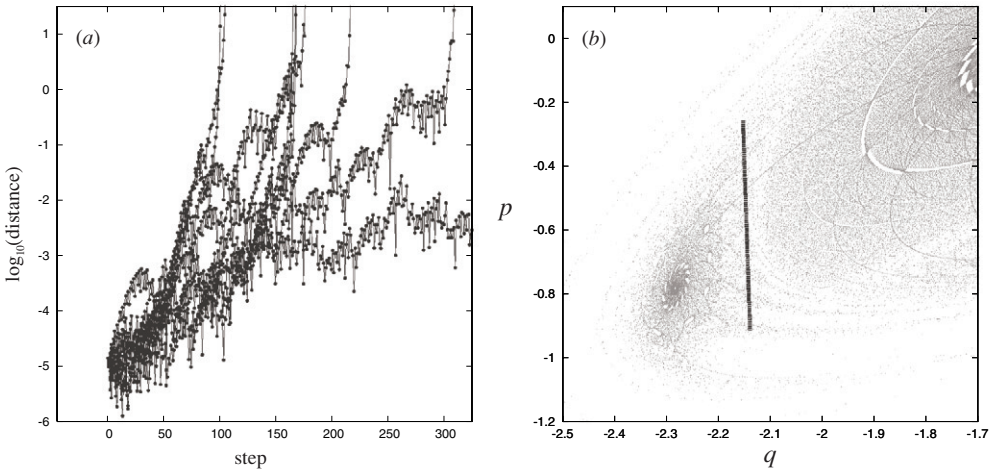

Figure 9. (*a*) The distance between the real plane and the trajectories that are initially located very close to the real plane. (*b*) The corresponding Poincaré map in $\mathbb{R}^2$. Ten initial points, which are taken inside the chaotic sea, are sampled very close to the thick line segment in (*b*). The quadratic map with $a = 0.644$ is used. The distance initially increases exponentially then explodes superexponentially in the limit of $n \to \infty$. The former behavior is common in any nonlinear maps, but the latter one is peculiar to the quadratic map.

set J^+ is defined as the boundary of the set K^+ of points whose forward orbits of a given map g remain in a finite region [28]

$$K^+ = \{(q, p) \in \mathbb{C}^2 : \{g^n(q, p)\}_{n>0} \text{ is bounded}\} \tag{32}$$

and

$$J^+ = \partial K^+. \tag{33}$$

If the map is invertible, both forward and backward iterations can be considered, for which we similarly define K^- as the set of points in $\mathbb{C}^2$ whose backward orbits are bounded. J^- is also defined as the boundary of K^- which we call the *backward Julia set*. The set $J \equiv J^+ \cap J^-$ is called the *Julia set* of g. On the Julia set J, the orbits have sensitive dependence on initial conditions, meaning that the chaotic motion is realized on it.

We will present numerical evidence that there exists a close connection between the Julia set and the Laputa chain. Since $J^\pm = \partial K^\pm$, it is not easy to single out the points only contained in $J^\pm$, we will compare the Laputa chain with the forward filled-in Julia set K^+. However, we note that further numerical studies, which will be done in our accompanying paper, strongly suggest that $J^\pm = K^\pm$. (See conjecture 3.3 of part II.)

Instead of making a direct observation of K^+ in $\mathbb{C}^2$, we here take the slice of K^+ in the initial plane $\mathcal{A}_\alpha = \{(q, p) \in \mathbb{C}^2 : p_0 = \alpha\}$ and compare the slice $K^+ \cap \mathcal{A}_\alpha$ with the set $\mathcal{M}_n^\alpha$. The slice of K^+ is numerically obtained by plotting the initial points whose trajectories remain in a ball of $\mathbb{C}^2$ with a certain finite radius.

In figures 10 (*a*) and (*c*), we show the set of initial points staying in a finite region up to the *n*th step

$$K_n^+ = \left\{(q_n, p_n) \in \mathbb{C}^2 : \sqrt{\left|p_n^2 + q_n^2\right|} < R\right\} \tag{34}$$

sliced by the initial plane, namely, $K_n^+ \cap \mathcal{A}_\alpha$. On the other hand, in figures 10(*b*) and (*d*) all the Laputa branches are displayed. Figures 10(*a*) and (*c*) show how small a fraction of the initial

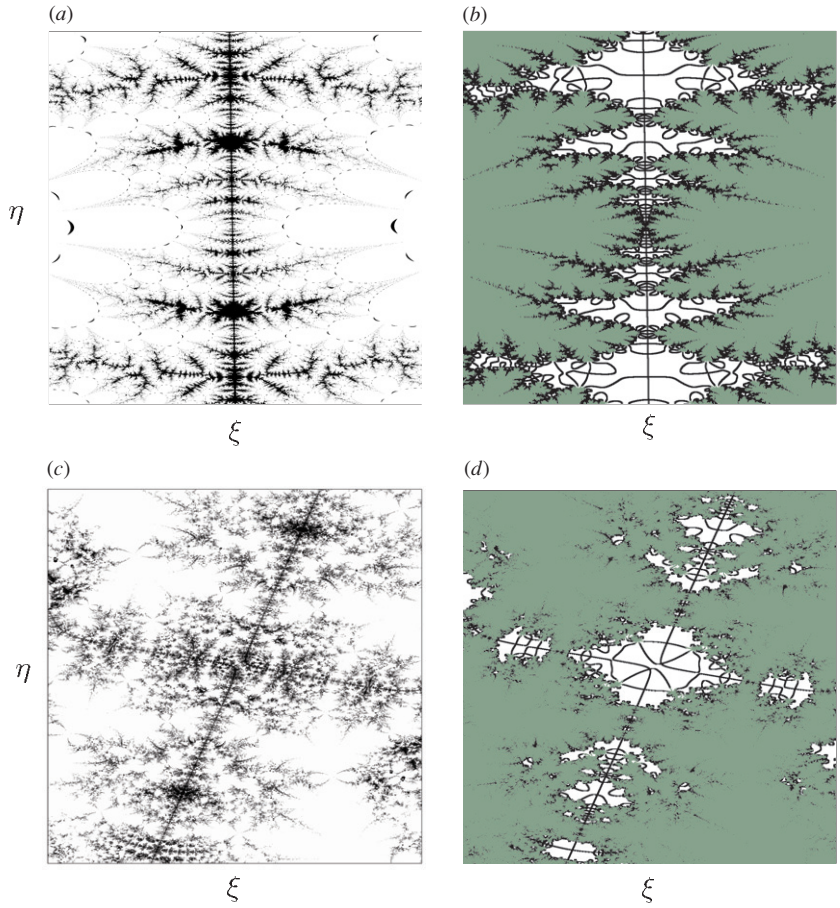

Figure 10. Slice of the filled-in Julia set K^+ for (*a*) the standard ($K = 1.5$) and (*c*) modified standard map ($K = 1.2$, $p_d = 5.0$ and $\omega = 1.0$). They are compared with the Laputa trunk chains shown by black lines in (*b*) (standard map) and (*d*) (modified standard map), respectively. The black lines are extracted out of the whole set (colored by green) according to the procedure mentioned in the text. The remaining Laputa branches are colored in green.

points remains in a finite region. This fact is closely connected with the fact that almost all the complex trajectories are repelled by the real plane and escape to infinity.

We pick up Laputa chains out of an enormous number of Laputa branches in $\mathcal{M}_n^\alpha$ by using the definition (1) plus (2) or (1) plus (2)′ presented in subsection 4.2. However, it is not easy to treat morphological convergence numerically, and so we examine whether the Laputa chains can be filtered by adopting the second conditions (2) or (2)′ only. First, let us consider a practical method to filter the initial points satisfying the condition (2). As described in subsection 4.5, if the trajectory does not approach exponentially to the real plane, it is exponentially repelled by the real plane. Hence, we can identify the trajectory approaching the real plane with the one whose end points have the distance from the real plane, i.e., $|\mathrm{Im}\, q_n|$, less than a certain small enough threshold value q_{th}, where the threshold value q_{th} is chosen appropriately. Similarly, we can identify the initial point of the trajectory satisfying the condition (2)′ with the one whose trajectory has imaginary part of action $|\mathrm{Im}\, S_n^{(\ell)}|$ less than a certain finite value S_{th}.

These two criteria work quite well: figures 10(*b*) and (*d*) show the subset of Laputa branches filtered out by applying the two criteria. Almost all of the points filling the (ξ, η)-plane are removed, and one finds that only the sets having the morphological feature peculiar to the trunk chain remain, and the remaining subsets coincide excellently with the set K_n^+. In this example the two conditions $|\mathrm{Im}\, q_n| < q_{\mathrm{th}}$ and $\left|\mathrm{Im}\, S_n^{(\ell)}\right| < S_{\mathrm{th}}$ are imposed to make sure the selection, but in practice either of the two criteria is sufficient for extracting the Laputa chains out of $\mathcal{M}_n^\alpha$, which means (2) and (2)′ plays an equivalent role.

5. Concluding remarks

As was reported in our previous papers [18, 21, 22], the initial points of complex trajectories dominating chaotic tunneling form particular sets which we called Laputa chains. These have a characteristic chain shape on the initial value plane. The present paper was devoted to providing more explicit characterizations of Laputa chains common to area-preserving maps, and in particular to clarifying the asymptotic nature of Laputa chains. What is important about the trajectories launched at a Laputa chain is that they approach exponentially to the real plane. Further, Laputa chains exhibit a strong tendency of convergence to asymptotic forms, and the imaginary part of the action along trajectories, which dominates the tunneling probability, also converges to finite values. Numerically confirmed features of Laputa chains were summarized as numerical observations (i)–(iii) in the text.

On the basis of (ii) and (iii), namely morphological convergency and the quasi-real-valuedness of the Laputa chains, we proposed an empirical definition of the Laputa chain. This definition will be developed into a mathematically more rigorous definition in the accompanying paper. These features are common to all the map systems that we explored in this paper, and so they are expected to be universal.

Chaotic regions in the real phase space in general repel the orbits close to the real plane. Nevertheless our observations show that the orbits starting at Laputa chains are destined for the real plane. This looks very peculiar. A plausible explanation for this is that in the asymptotic limit, the orbits starting from Laputa chains will stay on or very close to the complexified stable manifolds of unstable periodic orbits which are rich in the chaotic region in the real plane. We note that the key role of complexified stable manifolds has been confirmed even in a much more simple situation of two-dimensional barrier tunneling, where there is no chaos on the real plane but there exists only a single saddle as a dividing orbit [24, 21]. In this simple situation it can analytically be shown that the plateau structure characteristic in the tunneling wavefunction (see numerical observation (i) and figure 4) can directly be observed as a spectral feature of tunneling particles [40]. To the authors' knowledge, the role of the complexified stable manifold in multi-dimensional tunneling was first pointed out in [19, 20] for chaotic systems and in [24] for a non-chaotic system.

On the other hand, it is known that the stable manifolds of saddles approximate very well the (filled-in) forward Julia set K^+ namely, the set of initial points from which the trajectories in the forward iteration do not escape to infinity [43]. It is, therefore, quite natural to conjecture that the Laputa chains are closely related to K^+, and we indeed show numerical evidence exhibiting that the Laputa chain is well approximated by K^+, which typically exhibits a fractal structure.

The study of complex dynamical systems, initiated in classical papers by Julia and Fatou [45, 46], has made great progress in the last two decades [41–44]. In contrast to the mathematical study of real dynamical systems, which was driven by physical phenomena in celestial mechanics and statistical physics, the study of complex dynamical systems has been mainly motivated by purely mathematical interest. However, our findings show that results

from the theory of complex dynamical systems may be very relevant to physical phenomena, that is quantum tunneling.

We know that, both in integrable and nonintegrable limits, the invariant sets, the KAM curves in the former limit and unstable periodic orbits in the latter limit play central roles in developing the energy-domain semiclassical theory. However, the invariant sets so far considered in semiclassics have been confined to the real phase space. In order to incorporate the tunneling effect, it is quite natural that the relevant invariant sets should be extended to invariant sets in the fully complex phase space, especially Julia sets

The close connection between Julia sets and Laputa chains will be the focus of the next paper, where we provide more rigorous statements and analysis of the conjecture relating the mathematical theory of Julia sets in multi-dimensional complex dynamical systems and quantum tunneling in non-integrable systems. Detailed analyses developed there will lead us to a general hypothesis elucidating the nature of chaotic tunneling trajectories.

Acknowledgments

The authors thanks K Takahashi and T Onishi for many discussions throughout this study. They are also grateful to E Bedford for helpful comments and suggestions on multi-dimensional complex dynamical system theory. They express thanks to S Tsuji for offering a very nice lodging where they discuss the present subject intensively. This work is supported by the Grants-in-Aid for Scientific Research (C) no 20340100 from the Ministry of Education, Culture, Sports, Science and Technology of Japan.

Appendix A. Time-domain semiclassical propagator for general representations

We derive a semiclassical formula for the n-step propagator when arbitrary quantized invariant curves are taken as the initial and final manifolds. Here we confine ourselves to the case where the invariant curves are described by action-angle variables. We use the momentum representation of semiclassical propagator (12)

$$K_n^{sc}(p, p') = \sum_{\ell} A_n^{(\ell)}(p, p') \exp\left\{ \mathrm{i}\frac{S_n^{(\ell)}(p, p')}{\hbar} + \mathrm{i}\mu^{(\ell)}\frac{\pi}{2} \right\}, \tag{A.1}$$

with

$$S_n^{(\ell)}(p, p') = \sum_{j=1}^{n} \left[H_0\left(p_j^{(\ell)}\right) + V\left(q_{j-1}^{(\ell)}\right) + q_{j-1}^{(\ell)}\left(p_j^{(\ell)} - p_{j-1}^{(\ell)}\right) \right], \tag{A.2}$$

$$A_n^{(\ell)}(p, p') = \left[\frac{\partial^2 S_n^{(\ell)}(p, p')}{\partial p \partial p'} \Big/ 2\pi\hbar \right]^{1/2}, \tag{A.3}$$

where p, p' are used, instead of α, β, for labeling the initial and final momenta, respectively. $S_n^{(\ell)}$ and $A_n^{(\ell)}$ are computed for each trajectory $\left(q_j^{(\ell)}, p_j^{(\ell)}\right)(0 \leqslant j \leqslant n)$, which leaves p and reaches p' at 0- and n-steps, respectively, obeying the mapping rule (2). Below we drop the superscript $^{(\ell)}$ if there is no confusion.

Here we suppose that the initial and final quantum states are both quantized curves, which are parameterized by (φ', I'), respectively, in the classical limit. By taking actions as the parameters α and β specifying the initial and final manifolds introduced by equation (20), they are

$$\mathcal{A}_\alpha = \{(q, p) : q = q_i(I = \alpha, \varphi),\ p = p_i(I = \alpha, \varphi), \varphi \in \mathbb{C}\}, \tag{A.4}$$

$$\mathcal{B}_\beta = \{(q, p) : q = q_f(I' = \beta, \varphi'),\ p = p_f(I' = \beta, \varphi'),\ \varphi' \in \mathbb{C}\}, \tag{A.5}$$

where $q_{i,f}$ and $p_{i,f}$ are 2π periodic functions of φ and of φ'. A typical choice of initial manifold is to take the invariant curve of the linearized map around an elliptic fixed point of the map (2).

Let $|\alpha\rangle$ and $|\beta\rangle$ be the action eigenstates corresponding to the initial and final manifolds. Then its semiclassical momentum representation is expressed in terms of generating functions

$$\langle p|\alpha\rangle = \sqrt{-\frac{\partial^2 s_i(p,\alpha)}{\partial p \partial \alpha} \Big/ 2\pi \mathrm{i}\hbar}\, \exp\{\mathrm{i}s_i(p,\alpha)/\hbar\}, \tag{A.6}$$

$$\langle p'|\beta\rangle = \sqrt{-\frac{\partial^2 s_f(p',\beta)}{\partial p' \partial \beta} \Big/ 2\pi \mathrm{i}\hbar}\, \exp\big\{\mathrm{i}s_f(p',\beta)/\hbar\big\}, \tag{A.7}$$

where $s_{i,f}$ are generating functions, and the subscripts i and f are used below to indicate the initial and final manifolds, respectively.

Then the final semiclassical propagator connecting $\mathcal{A}_\alpha$ and $\mathcal{B}_\beta$ is computed simply by integrating over the intermediate variables p and p'

$$\hat{K}_n^{sc}(\alpha,\beta) = \int\int \mathrm{d}p'\,\mathrm{d}p \langle\beta|p'\rangle K_n^{sc}(p', p)\langle p|\alpha\rangle. \tag{A.8}$$

The integrations over p and p' are done using the ordinary saddle point approximation, deforming the integration paths so as to pass through the saddle points. First, the saddle points are determined by imposing the extremum condition on the total action

$$S_{\mathrm{tot}}(p, p') = -s_f(\beta, p') + S_n(p, p') + s_i(\alpha, p), \tag{A.9}$$

namely, $\partial S_{\mathrm{tot}}/\partial p = \partial S_{\mathrm{tot}}/\partial p' = 0$, which yields the new boundary conditions

$$\begin{aligned} &\frac{\partial S_n}{\partial p} - q_i = q(p, p') - q_i(\alpha, p) = 0, \\ &\frac{\partial S_n}{\partial p'} + q_f = -q'(p, p') + q_f(\beta, p') = 0. \end{aligned} \tag{A.10}$$

Here we used the basic relations of the generating function $S_n(p, p')$, $s_i(\alpha, p)$ and $s_f(\beta, p')$, i.e., equation (15) and

$$\begin{aligned} &\partial s_i(\alpha, p)/\partial p = -q, \quad \partial s_i(\alpha, p)/\partial \alpha = \varphi, \\ &\partial s_f(\beta, p')/\partial p' = -q', \quad \partial s_f(\beta, p')/\partial \beta = \varphi', \end{aligned} \tag{A.11}$$

respectively. Note that the coordinate q (or q') is regarded as a function of α (or β) and p, which is represented explicitly as $q_i(\alpha, p)$(or $q_f(\beta, p)$). Equations (A.10) require that the trajectory connecting p and p' should have the coordinates on the initial and final manifolds $\mathcal{A}_\alpha$ and $\mathcal{B}_\beta$ at initial and final steps, respectively. Thus all the trajectories now introduced are functions of α and β. Let the ℓth solutions of equations (A.10) be $p = \overline{p}^{(\ell)}(\alpha, \beta)$ and $p' = \overline{p}'^{(\ell)}(\alpha, \beta)$. Expanding S_{tot} around $\overline{p}^{(\ell)}$ and $\overline{p}'^{(\ell)}$ up to the second order, and integrating over p and p', we obtain

$$\hat{K}_n^{(sc)}(\alpha,\beta) = \sum_\ell \hat{\mathrm{A}}_n^{(\ell)}(\alpha,\beta) \exp\left\{\mathrm{i}\frac{\hat{S}_n^{(\ell)}(\alpha,\beta)}{\hbar} + \mathrm{i}\mu^{(\ell)}\frac{\pi}{2}\right\}, \tag{A.12}$$

where the new phase factor and amplitude factors are

$$\hat{S}_n^{(\ell)}(\alpha,\beta) = s_i(\alpha, \overline{p}^{(\ell)}) + S_n(\overline{p}^{(\ell)}, \overline{p}'^{(\ell)}) - s_f(\beta, \overline{p}'^{(\ell)}), \tag{A.13}$$

$$\hat{\mathrm{A}}_n^{(\ell)}(\alpha,\beta) = A_n(\overline{p}^{(\ell)},\overline{p}'^{(\ell)})\sqrt{\frac{\partial q_f(\beta,\overline{p}'^{(\ell)})/\partial\beta}{\det C\,\partial p_i(\alpha,\varphi)/\partial\varphi}}, \tag{A.14}$$

with C being the 2×2 matrix ($^{(\ell)}$ is omitted)

$$C = \begin{pmatrix} \partial^2 S_{\mathrm{tot}}(\overline{p},\overline{p}')/\partial\overline{p}^2 & \partial^2 S_{\mathrm{tot}}(\overline{p},\overline{p}')/\partial\overline{p}\partial\overline{p}' \\ \partial^2 S_{\mathrm{tot}}(\overline{p},\overline{p}')/\partial\overline{p}\partial\overline{p}' & \partial^2 S_{\mathrm{tot}}(\overline{p},\overline{p}')/\partial\overline{p}^2 \end{pmatrix}. \tag{A.15}$$

In the above derivation we have used equation (A.11). Substituting $p = \overline{p}(\alpha,\beta)$ and $p' = \overline{p}'(\alpha,\beta)$ into equation (A.10), and differentiating it by β with fixing α, we obtain

$$\det C = \frac{(\partial^2 S_n(\overline{p},\overline{p}')/\partial\overline{p}\partial\overline{p}')(\partial q_f(\overline{p}',\beta)/\partial\beta)}{\partial\overline{p}(\alpha,\beta)/\partial\beta}. \tag{A.16}$$

Substituting this into equation (A.14) and using equation (A.3), the final expression for the amplitude factor is

$$\hat{\mathrm{A}}_n^{(\ell)}(\alpha,\beta) = \left\{\frac{\partial\beta(\alpha,\varphi)}{\partial\varphi}2\pi\hbar\right\}^{-1/2} = \left\{-\frac{\partial\alpha(\beta,\varphi')}{\partial\varphi'}2\pi\hbar\right\}^{-1/2} = \sqrt{\frac{\partial^2\hat{S}_n^{(\ell)}(\alpha,\beta)}{\partial\alpha\partial\beta}\Big/2\pi\hbar}. \tag{A.17}$$

The last equation immediately follows from the relation confirming that the new action is a generating function:

$$\partial\hat{S}_n(\alpha,\beta)/\partial\alpha = \varphi,\ \partial\hat{S}_n(\alpha,\beta)/\partial\beta = -\varphi', \tag{A.18}$$

which are derived by differentiating equation (A.13) by α and β and making use of the extremum condition (A.10).

We often use the Cartesian coordinate q as the final manifold. In this choice $\mathcal{B}_\beta = \{(q,p) : q = \beta\}$, and action s_f should be such that

$$s_f(p,\beta) = -p\beta, \tag{A.19}$$

which immediately follows from $\langle p|\beta\rangle = \langle p|q\rangle = \sqrt{-1/2\pi\hbar\,\mathrm{i}}\,\mathrm{e}^{-\mathrm{i}pq/\hbar}$. For this choice φ' in equation (A.6) should be replaced by $-p'$, and relation (A.18) in this case should be read as

$$\partial\hat{S}_n(\alpha,\beta)/\partial\alpha = \varphi \qquad \partial\hat{S}_n(\alpha,\beta)/\partial\beta = p'. \tag{A.20}$$

The action-coordinate representation of the semiclassical propagator is used for the tunneling problem of the quadratic map (Hénon map).

Let (q_0,p_0) and (q_n,p_n) be the initial and final points of the trajectory, then equation (A.10) means that we now have to solve the boundary value problem by replacing $(q,p)\to(q_0,p_0)$ and $(q',p')\to(q_n,p_n)$ in equation (A.10), namely by setting

$$q_0 = q_i(\alpha,p_0), \qquad q_n(q_0,p_0) = q_f(\beta,p_n(q_0,p_0)),$$

where (q_n,p_n) are now looked on as the nth iterate of (q_0,p_0). This condition just requires that (q_0,p_0) and (q_n,p_n) are in $\mathcal{A}_\alpha$ and in $\mathcal{B}_\beta$, respectively. Therefore, the initial condition $(q_0,p_0)\in\mathcal{A}_\alpha$ is parameterized as $q_0 = q_i(\alpha,\varphi)$, $p_0 = p_i(\alpha,\varphi)$ by using the action-angle variables and the nth iterate of (q_0,p_0) can be thought of as a function of φ alone, which is denoted by $(q_n(\varphi),p_n(\varphi))$. Setting $\varphi = \xi + \mathrm{i}\eta$, the set-$\mathcal{M}$ should be defined by

$$\mathcal{M}_n^{\alpha,\beta} = \left\{(\xi,\eta)\in\mathbb{R}^2 : (q_n(\xi+\mathrm{i}\eta),p_n(\xi+\mathrm{i}\eta))\in\mathcal{B}_\beta\right\}, \tag{A.21}$$

and

$$\mathcal{M}_n^{\alpha} = \bigcup_{\beta\in\mathbb{R}}\mathcal{M}_n^{\alpha,\beta}. \tag{A.22}$$

The complexified angle variable $\varphi = \xi + \mathrm{i}\eta$ now plays the role of the search parameter.

The amplitude factor is nothing more than the derivative of p_n with respect to φ. It is also convenient to use the parametric expressions for the phase factors $s_i(\overline{p}, \alpha)$ and $s_f(\overline{p}', \beta)$ coming from initial and final states in terms of the associated angle variables

$$s_i = -\int^{\overline{p}} q(p)\,\mathrm{d}p = -\int^{\varphi} \mathrm{d}\varphi'' p_i(\alpha, \varphi'')\,\mathrm{d}q_i(\alpha, \varphi'')/\mathrm{d}\varphi'',$$
$$s_f = -\int^{\overline{p}'} q(p)\,\mathrm{d}p = -\int^{\varphi'} \mathrm{d}\varphi'' p_f(\alpha, \varphi'')\,\mathrm{d}q_f(\alpha, \varphi'')/\mathrm{d}\varphi''. \tag{A.23}$$

The phase factor $\mu^{(\ell)}$ together with the selection of the branch of the amplitude factor $\hat{\mathrm{A}}_n^{(\ell)}$ can practically be determined by analytically continuing the propagator along an appropriate path which is taken avoiding the unphysical regions on the (ξ, η)-plane, which are removed because of the Stokes phenomenon.

Appendix B. Some basic features of Laputa chains

In this appendix we describe some basic features of the Laputa chain. In particular we show that the close connection between adjacent branches forming a Laputa chain is due to quasi-real caustics.

First we explain what the smallness of the Laputa chain implies. The length scale in the initial plane is multiplied by the factor $\|Dg^n(p_0 = \alpha, q_0)\|$ in the time-evolved (q_n, p_n) space, and so the characteristic size s_n of the branch at the step n should be

$$s_n \sim 1/\mathrm{Max}(|\mathrm{d}p_n/\mathrm{d}q_0|, |\mathrm{d}q_n/\mathrm{d}q_0|) \tag{B.1}$$

if any dynamical structure with the length scale of O(1) corresponds to a branch in the Laputa chain. In particular, if chaotic dynamics is relevant, the size s_n decreases exponentially with n because of the exponential sensitivity of the trajectories. Indeed, the characteristic size of the branches constituting the Laputa chain decreases exponentially with n.

As shown in figure 2, each constituent branch in the Laputa chain is separated from an adjacent branch by a narrow gap whose size is much less than s_n. In such a gap, there always exists a caustic connecting the two branches. To understand this we consider the local behavior of the branch around a complex caustic specified by condition (26). Close to a caustic $q_0 = q_0^{(c)}$, we can expand

$$p_n - p_n^{(c)} = p_n^{(c)''}\big(q_0 - q_0^{(c)}\big)^2/2 + O\big(\big|q_0 - q_0^{(c)}\big|^3\big), \tag{B.2}$$

where $p_n^{(c)} = p_n\big(q_0^{(c)}, \alpha\big)$ and $'$ indicates derivative with respect to q_0 at $q_0 = q_0^c$. Take x, y as properly chosen local Cartesian coordinates around the caustic $q_0 = q_0^{(c)}$ on the complex q_0-plane. Scaling them by the size of the branch, we immediately obtain

$$xy = -\mathrm{Im}\, p_n^{(c)}\big|p_n^{(c)''}\big|^{-1} s_n^{-2}. \tag{B.3}$$

Equation (B.3) tells us that the branches around each caustic form a pair of hyperbola on the q_0 plane, as shown in figure 2. The distance between branches is given by $d_n = 2\sqrt{2}\big|\mathrm{Im}\, p_n^{(c)}\big|\big|p_n^{(c)''}\big|^{-1} s_n^{-2} \sim \big|\mathrm{Im}\, p_n^{(c)}\big|$ considering that $\big|\mathrm{d}^2 p_n(q_0)/\mathrm{d}q_0^2\big| \sim s_n^{-2}$, and so the narrowness of the gap means that $\big|\mathrm{Im}\, p_n^{(c)}\big| \ll 1$, which is due to the caustic being located close to the real plane.

References

[1] Balian R and Bloch C 1974 *Ann. Phys., NY* **85** 514
[2] Voros A 1983 *Ann. Inst. H. Poincare* A **39** 211

[3] Langer J S 1969 *Ann. Phys., NY* **54** 258
[4] Schulman L S 1981 *Techniques and Applications of Path Integration* (New York: Wiley)
[5] Miller W H 1970 *J. Chem. Phys.* **53** 1949
Miller W H 1974 *Adv. Chem. Phys.* **25** 69
[6] Davis M J and Heller E 1981 *J. Chem. Phys.* **75** 246
[7] Lin W A and Ballentine L E 1990 *Phys. Rev.* E **65** 2927
[8] Bohigas O, Tomsovic S and Ullmo D 1993 *Phys. Rep.* **223** 43
[9] Tomsovic S and Ullmo D 1994 *Phys. Rev.* E **50** 145
[10] Hensinger W K *et al* 2001 *Nature* **412** 52
[11] Mouchet A, Miniatura C, Kaiser R, Grémaud B and Delande D 2001 *Phys. Rev.* E **64** 016221
[12] Steck D A, Oskay W H and Raizen M G 2001 *Science* **293** 274
[13] Dembowski C, Gräf H -D, Heine A, Hofferbert A, Rehfeld H and Richter A 2000 *Phys. Rev. Lett.* **84** 867
[14] Brodier O, Schlagheck P and Ullmo D 2001 *Phys. Rev. Lett.* **87** 064101
Brodier O, Schlagheck P and Ullmo D 2002 *Ann. Phys., NY* **300** 88
[15] Doron E and Frischat S D 1995 *Phys. Rev. Lett.* **75** 3661
Frischat S D and Doron E 1998 *Phys. Rev.* E **57** 1421
[16] Creagh S C and Whelan N D 1996 *Phys. Rev. Lett.* **77** 4975
Creagh S C and Whelan N D 1999 *Phys. Rev. Lett.* **82** 5237
[17] Shudo A, Ishii Y and Ikeda K S 2009 *J. Phys. A: Math. Theor.* **42** 265102
[18] Shudo A and Ikeda K S 1995 *Phys. Rev. Lett.* **74** 682
Shudo A and Ikeda K S 1998 *Physica* D **115** 234
[19] Shudo A, Ishii Y and Ikeda K S 2002 *J. Phys. A: Math. Gen.* **35** L225
[20] Shudo A, Ishii Y and Ikeda K S 2008 *Europhys. Lett.* **81** 50003
[21] Onishi T, Shudo A, Ikeda K S and Takahashi K 2001 *Phys. Rev.* E **64** 025201
[22] Shudo A and Ikeda K S 1996 *Phys. Rev. Lett.* **76** 4151
[23] Shudo A and Ikeda K S 2008 *Nonlinearity* **21** 1831
[24] Takahashi K and Ikeda K S 2001 *Found. Phys.* **31** 177
Takahashi K, Yoshimoto A and Ikeda K S 2002 *Phys. Lett.* **297** 370
Takahashi K and Ikeda K S 2003 *J. Phys. A: Math. Gen.* **36** 7953
[25] Hénon M 1979 *Commun. Math. Phys.* **50** 69
[26] Friedland S and Milnor J 1989 *Ergod Theory Dyn. Syst.* **9** 67
[27] Gutzwiller M C 1990 *Chaos in Classical and Quantum Mechanics* (New York: Springer)
[28] Hubbard J H and Oberste-Vorth R W 1994 *Publ. Math. L'IHÉS* **79** 5
[29] Bedford E and Smillie J 1991 *Invent. Math.* **103** 69
[30] Bedford E and Smillie J 1991 *J. Am. Math. Soc.* **4** 657
[31] Bedford E and Smillie J 1992 *Math. Ann.* **294** 395
[32] Bedford E, Lyubich M and Smillie J 1993 *Invent. Math.* **112** 77
[33] Bender C M and Wu T T 1969 *Phys. Rev* **184** 1231
[34] Zinn-Justin J 1984 *Math. Phys.* **25** 549
[35] Silverstone H J 1985 *Phys. Rev. Lett.* **55** 2523
[36] Delabaere E, Dillinger H and Pham F 1993 *Ann. Inst. Fourier.* **43** 433
[37] Kawai T and Take Y 1998 *Algebraic Analysis of Singular Perturbation Theory (Translations of Mathematical Monographs)* (Providence, RI: American Mathematical Society)
[38] Berk H L, Nevins W M and Roberts K V 1982 *J. Math. Phys.* **23** 988
[39] Aoki T, Kawai T and Takei Y 1994 *Analyse algébrique des perturbations singuliéres: I* ed L Boutet de Monvel (Paris: Hermann) p 69
[40] Takahashi K and Ikeda K S 2005 *Europhys. Lett.* **71** 193
Takahashi K and Ikeda K S 2008 *J. Phys. A: Math. Theor.* **41** 095101
[41] Devaney R L 1989 *Introduction to Chaotic Dynamical Systems* 2nd edn (Reading, MA: Addison-Wesley)
[42] Beardon A F 1991 *Iteration of Rational Functions.: Complex Analytic Dynamical Systems* (Berlin: Springer)
[43] Morosawa S, Nishimura Y, Taniguchi M and Ueda T 1999 *Holomorphic Dynamics* (Cambridge: Cambridge University Press)
[44] Milnor J 1999 *Dynamics in One Complex Variable* (Braunschweig: Vieweg)
[45] Julia G 1918 *J. Math. Pure Appl.* **8** 47
[46] Fatou P 1906 *C. R. Acad. Sci. Paris* **143** 546